

X-672-72-122

PREPRINT

NASA TM X-65883

# INTERSTELLAR LINES IN THE ULTRAVIOLET SPECTRUM OF $\zeta$ OPH

(NASA-TM-X-65883) INTERSTELLAR LINES IN  
THE ULTRAVIOLET SPECTRUM OF ZETA OPH A.M.  
Smith (NASA) Apr. 1972 55 p CSCL 03B

N72-23895

G3/30 Unclass  
26837

ANDREW M. SMITH

APRIL 1972



— GODDARD SPACE FLIGHT CENTER —  
GREENBELT, MARYLAND

# INTERSTELLAR LINES IN THE ULTRAVIOLET SPECTRUM OF $\zeta$ OPH

ANDREW M. SMITH

NASA, Goddard Space Flight Center

Received \_\_\_\_\_

## ABSTRACT

Interstellar lines arising in  $C^0$ ,  $C^+$ ,  $O^0$ ,  $Si^+$ , and  $S^+$  observed in the ultraviolet spectrum of  $\zeta$  Oph by rocket spectrographic techniques are analyzed. The main results are that within a factor of 10 the abundances of  $C^+$ ,  $O^0$ , and  $Si^+$  outside the H II region surrounding  $\zeta$  Oph relative to the hydrogen abundance are equal to solar values. The lines in  $C^0$  and  $S^+$  imply that the interstellar matter is distributed among several clouds as indicated by high resolution visible spectra. The  $^2P_{3/2}^0$  (0.0079 eV) fine structure level of the ground state configuration in  $C^+$  is strongly populated, the abundance ratio of the  $^2P_{3/2}^0$  level to the  $^2P_{1/2}^0$  ground level being 1.5. It is suggested that the excited  $C^+$  ions are inside the Strömgren sphere where proton densities equal to or greater than  $220 \text{ cm}^{-3}$  can collisionally excite the ions at sufficient rates. Stellar absorption lines of C IV (1548.2, 1550.8Å) and N V (1238.8, 1242.8Å) are seen shifted to lower wavelengths indicating stellar mass loss. The stellar material will be stopped in the H II region by coulomb forces, and it is suggested that most of the  $C^+$  ions in

## I. INTRODUCTION

One of the prime objectives of sounding-rocket spectroscopy has been to obtain ultraviolet interstellar line spectra which arise in the abundant species of C, N, O, Si, S and Fe. Such observations require a hot background star which will provide sufficient flux against which the interstellar lines may be seen, and ideally, instrumental resolution of  $0.1\text{\AA}$  resolution or better. Perhaps the most satisfactory star for this purpose is  $\zeta$  Oph. It is a bright, 09.5 V star with a large rotational velocity equal to  $290\text{ km sec}^{-1}$  (Slettebak, 1956). The desirable consequence is that the confusion between stellar lines and interstellar lines is minimized. Furthermore, a recent and complete analysis of the visible interstellar spectrum of  $\zeta$  Oph (Herbig, 1968) is available for comparison purposes. According to Herbig the cloud structure is comparatively simple consisting of a strong  $-15\text{ km sec}^{-1}$  component and a weak  $-29\text{ km sec}^{-1}$  component. Under high resolution, however, these components show structure and additional components appear. The star is moderately reddened ( $E_{B-V} = +0.32$ ), and it exhibits a rich molecular spectrum in the visible spectral range. Thus, it is reasonable to expect that ultraviolet molecular band systems such as those of  $\text{H}_2$  and CO will appear in the spectrum.

An ultraviolet spectrum of  $\zeta$  Oph from 1150 to  $1700\text{\AA}$  with the moderate resolution of  $0.5\text{\AA}$  has been obtained by this

laboratory. Despite the fact that the planned for resolution of  $0.1\text{\AA}$  was not attained interstellar lines due to  $\text{C}^0$ ,  $\text{C}^+$ ,  $\text{O}^0$ ,  $\text{Si}^+$ , and  $\text{S}^+$  are clearly present as are those of the fourth positive system of CO which have been reported earlier (Smith and Stecher, 1971). The analysis of atomic and ionic lines constitutes the subject matter of this paper, and although the accuracy of the results is poor due to the limited resolution it is possible to reach some interesting tentative conclusions.

## II. EXPERIMENT

The instrument consists of two one-meter Wadsworth-type spectrographs in which spherical gratings serve as the objective as well as the dispersive components. One of these, intended to record the  $\zeta$  Oph spectrum from 900 to  $1450\text{\AA}$ , did not operate properly. The other provided an unwidened spectrum extending from 1162 to  $1710\text{\AA}$  with a nearly linear dispersion of  $4.51\text{\AA mm}^{-1}$  and a resolution of about  $0.5\text{\AA}$ . The spectrogram was recorded on Kodak 101-01 film which was exposed for 188 sec at a mean altitude of 144 km. Subsequently, the data were reduced to a relative flux distribution with wavelength, the wavelength scale being determined by a quadratic fit of observed features to the stellar lines of C III ( $1247.37\text{\AA}$ ), Si IV ( $1402.77\text{\AA}$ ), and He II ( $1640.43\text{\AA}$ ). Through consistency checks made with identified lines the accuracy of the assigned wavelength scale should be better than  $\pm 0.1\text{\AA}$  between 1247 and  $1640\text{\AA}$ .

### III. DISCUSSION OF THE DATA

Segments of the reduced data are presented in Figure 1. In each segment a wavelength scale of  $1\text{\AA} \text{ div}^{-1}$  is plotted on the axis of the abscissas, and a relative flux scale is plotted on the axis of the ordinates. The relative flux scales are not necessarily the same in each segment, and the axis of the abscissas does not represent the zero-flux level. The dashed lines indicate the assumed value of the background stellar radiation.

The first two segments show strong absorption lines with half-widths of about  $0.6\text{\AA}$  which can be attributed to the triplet resonance lines of S II ( $1250.5$ ,  $1253.8$ ,  $1259.5\text{\AA}$ ). On close inspection the lines show a shift toward shorter wavelengths of approximately  $0.1\text{\AA}$  from the laboratory values which corresponds to a radial velocity of  $-34 \text{ km sec}^{-1}$ . This shift is particularly evident for the  $1253.8$  and  $1259.5\text{\AA}$  lines. Apart from a possible contribution to the  $1253.8\text{\AA}$  feature from an interstellar P I ( $1253.7\text{\AA}$ ) line there are no other reasonable identifications for these lines. As is shown in Section IV the column density of  $\text{S}^+$  ions calculated on the assumption that all of the absorption arises either in one cloud or in two is far greater than would be expected on the basis of the measured column density of hydrogen atoms and an assumed solar S/H abundance ratio. It becomes plausible to assume, at least temporarily, that the  $\text{S}^+$  ions are more widely distributed in space and velocity than the double-cloud model would imply. Such

an assumption would help to explain the shortward shift of the observed lines, and would make possible the derivation of considerably smaller  $S^+$  ion column densities on the basis of the measured resonance line equivalent widths.

None of the other lines shown in Figure 1 are completely symmetric about their minima, but with the exception of the C I (1280.1Å) and C I (1328.8Å) blends their minima show good correlation with laboratory wavelengths. It is difficult to say whether the difference between the implied radial velocities of the  $C^0$  and  $S^+$  particles on one hand and the  $C^+$ ,  $O^0$  and  $Si^+$  particles on the other reflect a real difference in the location and velocities of the particles or is simply the result of differing strengths of the components which contribute to the observed feature. In this regard it will be shown in Section IV that the equivalent widths of the C II, O I, and Si II lines lie on the square-root part of the curve of growth, while those of C I and S II lie near or on the flat part of the curve of growth. Perhaps all that can be said is that there is probably some structure in the C I and S II lines related to the velocity and spatial distribution of the  $C^0$  atoms and  $S^+$  ions which will be revealed only when a spectrogram of greater resolution is obtained.

The stellar spectrum itself must contain to some extent the resonance lines of the singly ionized species. Thus, the broad dip in the spectrum delineated by the dashed line and centered on 1335.2Å is to be associated with the stellar

C II ( $1334.5$ ,  $1335.7\text{\AA}$ ) lines. These lines do not appear in the appropriate stellar model spectra of Bradley and Morton (1969), and are presumably weak. Therefore, because of the type of star and because of the broadening of stellar lines ( $\sim 1.3\text{\AA}$ ) due to the high rotation of the star it seems reasonable to place the stellar background as shown. In the case of the C I ( $1328.8\text{\AA}$ ) blend it was difficult to fit a smooth background line to the gross features of the spectrum; a straight horizontal line was used instead. There is reason to suspect, however, that the feature centered on  $1329\text{\AA}$  is due in part to  $\text{Si}^{++}$  ions in the stellar atmosphere through the predicted Si III ( $1328.8\text{\AA}$ ) line, and the original expectation that this absorption feature was due exclusively to carbon atoms is consequently in doubt.

Likewise, the asymmetrical feature near  $1280\text{\AA}$  which is primarily due to a C I blend is probably also formed in part by a stellar Si III ( $1280.4\text{\AA}$ ) line with a possible contribution from a stellar Fe IV ( $1280.4\text{\AA}$ ) line. A measurement of an equivalent width was not attempted in this case. No identifications other than a blend of C I lines have been made for the feature centered on  $1277.2\text{\AA}$ . The feature is obviously asymmetric, and to estimate the equivalent width only the long wavelength side of the feature was used. The area measured is indicated by the cross-hatching.

The same procedure has been followed in the cases of the Si II ( $1260.4\text{\AA}$ ), Si II ( $1304.4\text{\AA}$ ), and O I ( $1302.2\text{\AA}$ ) lines. In the first case, the long wavelength side of the profile is

influenced by the (9-0) vibrational transition of the fourth positive system of  $C^{12}O^{16}$  (Smith and Stecher, 1971) and a Si III (1301.2 $\text{\AA}$ ) line. In both the asymmetric and the symmetric features the areas used in the equivalent width determinations are indicated by cross-hatching.

The  $L\alpha$  line is observed in absorption on the same spectrogram as the lines of the heavier elements and is effectively due to interstellar hydrogen atoms. A rectified flux distribution in the vicinity of 1215.7 $\text{\AA}$  which includes several features found in the wings of the  $L\alpha$  line is shown in Figure 2. The equivalent width and column density of hydrogen atoms are found by fitting a computed contour shown by the dashed line to the observed rectified profile as discussed previously (Smith, 1970).

The equivalent widths of the lines and blends discussed above are listed in the second column of Table 1. The quoted uncertainties reflect only a maximum uncertainty in the level of the stellar background flux.

#### IV. COLUMN DENSITIES

In general, the curve of growth procedures described by Strömgren (1948) were followed in order to derive column densities. In the case at hand, all the data points lie on or between the flat portion and the square-root portion of the appropriate curve of growth, and this necessitates a computation of a curve of growth for each line or blend of closely spaced lines as in the case of the CI multiplets.

To illustrate the procedure we show in Figure 3 the computed curves of growth for the C II (1334.5Å) and C I (1277.2Å) lines. Plotted on the abscissa is  $\log \tau_0$  where  $\tau_0$  is the optical depth in the center of the line and is given by the expression

$$\tau_0 = N \frac{\pi^{1/2} e^2}{mc^2} f \frac{\lambda^2}{b_\lambda} \quad (1)$$

In this expression  $N$  is the number of absorbers  $\text{cm}^{-2}$ ,  $f$  is the oscillator strength and  $b_\lambda$  is equal to  $(\lambda/c)(2kT/Am_0)^{1/2}$ . As usual  $k$  is the Boltzman constant,  $T$  the temperature, and  $Am_0$  the mass of the atom or ion. In this case we set  $b \equiv (2kT/Am_0)^{1/2} = 1.5 \text{ km sec}^{-1}$  which is the value determined by Herbig (1968) from fitting the Ca II H and K lines to Strömgren's curve of growth. Plotted on the ordinate is  $\log (W/b_\lambda)$  where  $W$  is the equivalent width of an absorption line formed by  $N$  absorbers  $\text{cm}^{-2}$ . The optical depth in a line,  $\tau(\lambda)$ , was calculated using the Voigt-function together with  $\tau_0$ . For blends  $\tau(\lambda)$  was simply the sum of the  $\tau(\lambda)$ 's for each line. From the optical depths residual intensities were computed and a subsequent integration

produced the desired equivalent widths. Thus, Doppler line broadening and radiation damping were included in the curve of growth computations. The effects produced by radiation damping are of primary importance in analyzing the present data. All oscillator strengths were taken from the publication of Wiese, Smith and Glennon (1966) and Wiese, Smith, and Miles (1969).

Two curves for each line are shown to illustrate the difference between the assumptions of a single-cloud model and a double-cloud model. In the latter case 83% of the absorbers were in one cloud and 17% in the other, the proportions being estimated on the basis of the relative strengths of the Ca II lines in the  $-15$  and  $-29$  km sec $^{-1}$  clouds observed by Herbig (1968). The data points reduced to  $\log (W/b_\lambda)$  with  $b = 1.5$  km sec $^{-1}$  are plotted on the single-cloud curves. The boxes surrounding the data points indicate the magnitude of the uncertainty due to locating the stellar background flux (vertical dimension), and the effect of the uncertainty in the oscillator strengths (horizontal dimension). The column density of  $C^+$  ions in the  $2p_{1/2}^o$  ground state corresponding to the horizontal position of the data point as shown is  $(1.4^{+0.5}_{-0.3}) 10^{17}$  cm $^{-2}$ . The location of the data point well up on the square root portion of the curve of growth suggests that the asymptotic expression giving the equivalent width of a line in terms of the square root of the absorber column density could be used. The appropriate equation as given by Stone and Morton (1967) is

$$W = \frac{2\pi e^2}{M_e c^2} \lambda \left( 2N \frac{f_{Lu}}{g_u} \sum_l g_l f_{lu} \right)^{1/2} \quad (2)$$

where the transition occurs from the lower level  $L$  to the upper level  $u$  with statistical weight  $g_u$  which is broadened by spontaneous decays to lower levels  $l$  with statistical weights  $g_l$ . The sum is carried out over all permitted transitions with  $l < u$ . As a check on the column density of  $C^+$  ions in the  $2P_{1/2}^o$  state determined by the curve of growth method the appropriate quantities were inserted in equation (2) with the result that  $N = 1.4 \times 10^{17} \text{ cm}^{-2}$ , i.e. both methods produce the same result well within the limits imposed by the uncertainties. This calculation shows that for  $b = 1.5 \text{ km sec}^{-1}$  equation (2) will yield sufficiently accurate answers, and further, that a distinction between single and double clouds is not meaningful for the C II (1334.5, 1335.7 $\text{\AA}$ ) lines in view of the uncertainties in the equivalent widths. Using Figure 3 one can show that when the uncertainties are ignored the column density of  $C^+$  ions in the  $2P_{1/2}^o$  state for the double-cloud model is a factor of 1.3 less than in the case of the single cloud model. Herbig (1968) has derived a value for  $b$  of  $2.4 \text{ km sec}^{-1}$  from a fit of the Na I (3302.4, 3303.0 $\text{\AA}$ ) and Na I (5890.0, 5895.9 $\text{\AA}$ ) doublets to Strömgren's curve of growth. If this value of the turbulence parameter is used the  $C^+$  ion column density is reduced by a factor of 2.5 and equation (2) is no longer valid.

The C II (1335.7 $\text{\AA}$ ) line which originates in the ground state  $2P_{3/2}^o$  level and the resonance lines of Si II (1260.4 $\text{\AA}$ ),

Si II (1304.4 $\text{\AA}$ ), Si II (1526.7 $\text{\AA}$ ) and O I (1302.2 $\text{\AA}$ ) were all analyzed in the same way as the C II (1334.5 $\text{\AA}$ ) line using curves of growth computed for each line and a turbulence parameter equal to  $1.5 \text{ km sec}^{-1}$ . The resulting column densities for all these lines are listed in the third and fourth columns of Table 1. In each case the reduction in column densities resulting from a change of interpretation on the basis of a single-cloud model to a double-cloud model is relatively small, a factor of 2 or less, and within the listed uncertainties.

Such is not the case for the C I and S II resonance lines. It seems likely in view of the shape of the spectral features identified with C I lines that several lines of each multiplet are present in a blend which is either intrinsic or induced by the instrumental profile. For an initial estimate of the strength of each line involved in the C I (1277.2 $\text{\AA}$ ) and C I (1328.8 $\text{\AA}$ ) multiplets it was assumed that the lower levels were populated by collisions and that the population of a given level  $i$  relative to the ground level  $o$  is given by  $n_i/n_o = (g_i/g_o) \exp(-\chi_i/kT)$  where the  $n_i$  is the number density of atoms in energy level  $i$ , and  $\chi_i$  is the excitation energy of level  $i$ . The carbon atom has three fine structure levels in the  $^3\text{P}$  ground state configuration with excitation energies of 0.0000, 0.0020 and 0.0054 eV for which  $J = 0, 1$ , and  $2$  respectively. If  $T = 100^\circ\text{K}$  the fraction of atoms in the  $J = 2, 1$ , and  $0$  levels respectively is 0.44, 0.39, and 0.17. With this information curves of growth for the C I (1277.2 and C I (1328.8 $\text{\AA}$ ) multiplets and for both the single and double-cloud models may be computed. Although in the case of a blend

$\tau_0$  loses its usual significance it may be defined such that the linear part of a curve of growth computed for a blend of C I lines coincides with the linear part of a curve of growth computed for a single line. This normalizing procedure has been followed in plotting the computed curves of growth for the C I (1277.2Å) blend shown in Figure 3. The results of this analysis for both the C I (1277.2Å) and C I (1328.8Å) blends and for both the single and double cloud models are given in columns 3 and 4 of Table 1. If all the carbon atoms were in one cloud the uncertainties permit a reduction in the listed column density corresponding to the C I (1277.2Å) multiplet by a factor of 45. If the carbon atoms are distributed between two clouds according to the recipe given above the resulting column density is 40 times less than in the single-cloud case and the uncertainties could increase this factor to 200. Thus the column density of the carbon atoms is very uncertain and quite dependent on the model used for analysis.

The S II resonance lines are puzzling; the equivalent widths of these lines are quite large as are those of the C I resonance lines, but the strength of the S II lines cannot be explained either by the experimental uncertainties or by assuming that the  $S^+$  ions are distributed as prescribed by the double-cloud model. Analyzing the data using the curve of growth method described above the column densities listed in Table 1 for both the single and double-cloud models were derived; they are much too large if one expects the interstellar abundances to be approximately those found in the sun. For example, the

the equivalent width of the S II (1259.5Å) line yields a  $S^+$  ion column density of  $1.4 \times 10^{19} \text{ cm}^{-2}$ . The column density of hydrogen atoms as previously determined (Smith and Stecher, 1971) from the  $L\alpha$  line is  $(4.6 \pm 1.5) 10^{20} \text{ cm}^{-2}$ . Thus, the approximate sulfur to hydrogen abundance ratio averaged over the distance from the earth to the nearest boundary of the  $\zeta$  Oph Strömgren sphere is  $3.0 \times 10^{-2}$  which is to be compared to the solar value of  $2.0 \times 10^{-5}$  (Goldberg, Müller, and Aller, 1960). As in the case of the carbon atoms the uncertainties in the column densities of the  $S^+$  ions in the double-cloud model are large due to the fact that the  $\log (W/b_\lambda)$  values lie close to the saturated part of the curve of growth. However, the uncertainties only permit a maximum reduction in the measured sulfur to hydrogen abundance ratio to a value which is still a factor of 10 larger than the solar abundance ratio.

It is possible to apply the doublet ratio method to the 1250.5 and 1253.8Å lines of S II since both lines arise from the same level. Use of this method implies that the equivalent width of the S II (1259.5Å) line is in error since the line has the smallest measured equivalent width and yet the largest  $f$ -value. The resulting  $S^+$  ion column density is  $3.7 \times 10^{17} \text{ cm}^{-2}$  which gives an abundance ratio of  $8.0 \times 10^{-4}$ . The derived turbulence parameter,  $b$ , is  $6.7 \text{ km sec}^{-1}$  which is considerably greater than the largest value for  $b$  ( $2.4 \text{ km sec}^{-1}$ ) found by Herbig (1968). The ratio of the equivalent widths of these two lines, however, is sufficiently uncertain to permit the larger column densities and small turbulence parameter determined

by the first method, and therefore little insight is gained by using the doublet ratio method.

In view of these results it seems likely that the observed S II features are due to an unknown number of component lines which the instrument is unable to resolve, but which unfortunately has a most critical effect on the derivation of the  $S^+$  ion column densities.

While the determination of the oxygen atom column density is accomplished by the methods discussed above, the question arises as to how much of the oxygen is located in the earth's atmosphere above the rocket. The simplest approach in answering this question is to integrate a model distribution of oxygen in the earth's exosphere outward from an appropriate mean altitude to obtain a telluric contribution to the total oxygen column density. For this purpose the summer-time model with an exospheric temperature of  $1500^{\circ}\text{K}$  contained in the "U.S. Standard Atmosphere Supplements" (1966) was used. The column density of all the residual atomic oxygen obtained when the integration starts at the mean altitude of 144.5 km achieved during exposure is  $6.7 \times 10^{16} \text{ cm}^{-2}$ . Stone and Morton (1967) estimate that 62% of this oxygen is in the  $^3\text{P}_2$  ground state from which the O I ( $1303.2\text{\AA}$ ) arises. Consequently, the telluric contribution becomes  $4.2 \times 10^{16} \text{ cm}^{-2}$  which is 2% of the column density determined on the basis of a single-cloud model.

## V. LINE-OF-SIGHT INTERCLOUD GAS DISTRIBUTION

In order to analyze the data further it is necessary to obtain a model distribution of the inter-cloud gas in both the H I and H II regions. The procedure discussed by Herbig (1968) is followed closely here where one of his models with the following characteristics is used. The radius of the H II region surrounding  $\zeta$  Oph is 15 pc within which the density of hydrogen ions and electrons is equal to  $3 \text{ cm}^{-3}$ . According to Herbig (1968) these values are compatible with the data afforded by direct photography of the emission region surrounding  $\zeta$  Oph and radio observations. Outside the ionization front a shell of hydrogen with a density of  $3 \text{ cm}^{-3}$  and an electron to hydrogen atom density ratio,  $\epsilon$ , of  $6 \times 10^{-4}$  extends to 20pc. From 20 to 170pc, i.e. to the sun,  $\epsilon$  remains the same and the hydrogen atom density is  $0.07 \text{ cm}^{-3}$ . The electrons are presumed to arise from the photoionization of C, Mg, Si, and Fe which are present with solar abundances. The average hydrogen atom density along the extended 20 to 170pc path is reduced somewhat from Herbig's value of  $0.1 \text{ cm}^{-3}$ , reflecting a heavy reliance on rocket results (Jenkins, 1969) for determining typical intercloud densities. The temperature inside the H II region is  $10^4 \text{ (K)}$ , and outside the H II region is  $10^2 \text{ (K)}$ . This model corresponds to one of the three which Herbig (1968) discusses with the omission of an interstellar cloud in which most of the visible spectrum arises.

The column densities of atoms or ions in these three

extra-cloud regions may be found by performing the integrations designated in equations (13a, b) of Herbig (1968). When the case of carbon is considered these equations become

$$N(C^0) = R(C) \int n^3(H) \frac{\epsilon^2}{D} dr, \text{ and} \quad (3a)$$

$$N(C^+) = R(C) \int n^2(H) \frac{\epsilon h_1}{D} dr \quad (3b)$$

where

$$D = \epsilon^2 n^2(H) + h_1 \epsilon n(H) + h_1 h_2. \quad (3c)$$

Here,  $n(H)$  is the hydrogen atom density and  $R(C)$  is the solar C/H abundance ratio. The quantity  $h_1$  is defined as:

$$h_1 \equiv \frac{n(C^+)}{n(C^0)} n(e) = \frac{\Gamma}{\alpha} \quad (4)$$

where  $n(C^+)$  and  $n(C^0)$  are the number densities of singly ionized and neutral carbon atoms respectively,  $n(e)$  is the number density of electrons,  $\Gamma$  is the photoionization probability per atom  $\text{sec}^{-1}$ , and  $\alpha$  is the recombination coefficient in units of  $\text{cm}^3 \text{sec}^{-1}$ . The quantity  $h_2$  is related to the number density ratio of doubly to singly ionized carbon,  $n(C^{++})/n(C^+)$ , in the same manner. The integrations in equations (3a, b) are to be carried out over the range of distances appropriate to the three different regions.

The value of  $\Gamma$  may be calculated from Herbig's equation (8) reproduced here as:

$$\Gamma = 10^{-8} h^{-1} \int_0^\lambda a_\lambda u d\lambda. \quad (5)$$

where  $h$  is Planck's constant,  $a$  is the photoionization cross-section,  $u$  is the energy density, and  $\lambda_0$  is the threshold for photoionization. The wavelengths are in Angstrom units. The energy density is comprised of two components, one due to the general galactic background, and the other due to the star. The energy density of the galactic background was determined from the results of Habing (1968). In order to estimate the stellar component of the energy density a line blanketed model of Bradley and Morton (1969) with  $T_e = 28640$  ( $^{\circ}\text{K}$ ) and  $\log g = 4.0$  was used. The stellar radius was assumed to be  $8R_{\odot}$ , and the integrations in equation (5) started at  $227.8\text{\AA}$ , the onset of the He II continuum. The photoionization cross-sections were calculated for all atoms and ions with the exception of Si and  $\text{Si}^+$  from formulas given by Seaton (1958). For Si and  $\text{Si}^+$  similar formulas of Chapman and Henry (1971) were used.

The recombination coefficient for atomic oxygen (final state) with  $T = 10^4$  ( $^{\circ}\text{K}$ ) was kindly provided by Dr. R. Kirkpatrick. Seaton's (1951) values for atomic carbon at  $10^2$  ( $^{\circ}\text{K}$ ) and  $10^4$  ( $^{\circ}\text{K}$ ) were used, and recombination coefficients at these two temperatures for singly ionized carbon were calculated on the basis of formulas given by Silk and Brown (1971). Hydrogenic values were used for all other recombination coefficients required. Table 2 summarizes the results. Typical values of  $\Gamma$  for each atom or ion of interest at varying distances from the star are listed in the columns. The recombination coefficients are listed at the end of the columns for which they apply.

The photoionization coefficients for  $C^+$ ,  $Si^+$ ,  $O^0$ , and  $O^+$  are set equal to zero outside the H II region since their ionization potentials are greater than that of hydrogen, and the energy density of extreme ultraviolet radiation ( $\lambda < 200\text{\AA}$ ), X-rays, and cosmic rays can for our present purpose be ignored.

Using the model parameters and the values of  $\Gamma$  and  $\alpha$ , for which typical values are presented in Table 2, the integrations in equations (3a, b) were performed. The resulting column densities are listed in Table 3 for each of the three regions through which the line-of-sight passes. This model distribution of atoms and ions will be used in the following sections to correct the measured column densities for contributions from the intercloud medium. In some cases the corrections are small and errors in the model are unimportant. In other cases, particularly that of  $C^+$ , the corrections are large, and knowledge of the correct distribution of the intercloud gas is important. Consequently, the column density of  $C^+$  ions inside a cloud determined from the present observation is quite uncertain.

## VI. POPULATION OF THE $2P^0_{3/2}$ LEVEL OF THE $C^+$ IONS

The strength of the C II (1335.7Å) line is remarkable in that it represents absorptions from the excited, 0.0079 eV,  $2P^0_{3/2}$  fine structure level of the ground state which, therefore, must be strongly populated. This is borne out by the results presented in Table 1. The radiative decay of this level has been recognized as an important cooling mechanism for interstellar clouds (e.g. Penston, 1970, and references appearing therein), but such a large population of the excited level was not altogether expected. Another observation relevant to the excitation of the  $C^+$  ions is that a similar level in  $Si^+$  ions at 0.036 eV is not appreciably populated since no obvious lines arising from this excited level appear in the spectrum. If it is assumed that the excitation of the  $C^+$  ions is achieved by collisions with gas particles then by setting the mean energy per gas particle,  $\frac{3}{2} kT$ , equal to the fine structure level excitation a lower limit to the gas temperature may be estimated; this limit is 61°K. In addition to the fact that the C II (1334.5, 1335.7Å) lines are narrow, i.e. close to the limiting instrumental resolution of 0.5Å, the apparent absence of  $Si^+$  ions excited to the 0.036 eV,  $2P^0_{3/2}$  level seems to rule out the possibility that the C II lines are formed in the stellar atmosphere.

The density of the gas may be estimated if it is assumed that the excitation is accomplished through collisions of  $C^+$  ions with hydrogen atoms and electrons in the case of an H I region and with protons and electrons in the case of an H II region. This neglects collisional excitation due to  $H_2$  molecules

for which cross-sections are unknown to the author. The observed population ratio of the  $^2P_{3/2}^0$  to  $^2P_{1/2}^0$  levels in  $C^+$  ions is related to the excitation and de-excitation rates by the equation

$$\frac{Q(\frac{1}{2}, \frac{3}{2})}{Q(\frac{3}{2}, \frac{1}{2}) + w(\frac{3}{2}, \frac{1}{2})} = \frac{N'(C_{3/2}^+)}{N'(C_{1/2}^+)} \quad (7)$$

where  $Q(\frac{1}{2}, \frac{3}{2})$  is the total collision excitation rate,  $Q(\frac{3}{2}, \frac{1}{2})$  is the total collision de-excitation rate, and  $w(\frac{3}{2}, \frac{1}{2})$  is the radiative decay rate. The quantities  $N'(C_{3/2}^+)$  and  $N'(C_{1/2}^+)$  are the column densities of  $C^+$  in the  $^2P_{3/2}^0$  and  $^2P_{1/2}^0$  levels respectively within a cloud, i.e. the observed column densities corrected for contributions from the intercloud medium.

Electron cross-sections were computed from equation (14) of Bahcall and Wolf (1968) which is reproduced here as

$$\langle \sigma v \rangle_e = \frac{(8.63 \times 10^{-8} \text{ cm}^3 \text{ sec}^{-1}) \Omega(\frac{1}{2}, \frac{3}{2})}{T_4^{1/2} g_{1/2}} \quad (8)$$

Here,  $\langle \sigma v \rangle_e$  is the value of  $\sigma v$  averaged over a Maxwellian velocity distribution,  $\Omega(\frac{1}{2}, \frac{3}{2})$  is the transition collision strength,  $T_4$  is the temperature in units of  $10^4(^{\circ}\text{K})$  and  $g_{1/2}$  is the statistical weight of the  $^2P_{1/2}^0$  level. For upward transitions the right side of equation (8) must be multiplied by  $\exp(-\chi/kT)$  where  $\chi$  is the excitation energy. From the principal of detailed balance the downward rates may be obtained

by dividing the right side of equation (8) by  $g_{3/2}/g_{1/2}$ . For the quantity  $\Omega(\frac{1}{2}, \frac{3}{2})$  a value of 1.44 was used which was taken from Table 4 of Bahcall and Wolf (1968).

Calculations of the excitation cross-section due to collisions with hydrogen atoms at various center-of-mass energies have been made by Weisheit and Lane (1971). It was necessary to average their computed values of  $\sigma v$  over a Maxwellian velocity distribution, and this computation was complicated by the necessity of obtaining the threshold value of  $\sigma$  through extrapolation. Nevertheless, the value of  $\langle \sigma v \rangle$  for upward transitions was obtained in this way, and for downward transitions the upward rate was divided by  $(g_{3/2}/g_{1/2}) \exp(-\chi/kT)$ . The results of these calculations are summarized in Table 4 which contains the collision rates per hydrogen atom due to both electrons and hydrogen atoms. In order to relate the electron collision rate to the hydrogen atom density, we have assumed that the ratio of the electron density to the hydrogen atom density is  $6 \times 10^{-4}$ .

Now, to obtain the ratio of  $N'(C_{3/2}^+)/N'(C_{1/2}^+)$  it is necessary to correct the derived column densities appearing in Table 1 for contributions from regions outside the cloud. A preliminary calculation of collision rates shows that there is no substantial excitation of the  $J = 3/2$  level outside the cloud in either the H II or H I regions since the densities in these regions are far too low. Thus, no correction need be made in the case of the excited ions, thus  $N'(C_{3/2}^+) = N(C_{3/2}^+)$ . Making

use of the column densities of Table 3 and the derived value for  $N(C_{1/2}^+)$  in Table 1 we find that  $N(C_{1/2}^+) = 0.44 \times 10^{17} \text{ cm}^{-2}$ . The ratio,  $N'(C_{3/2}^+)/N'(C_{1/2}^+)$ , is therefore equal to 2.3. This ratio is not possible since the maximum possible population ratio of the fine structure levels occurs in the thermal equilibrium limit and is equal to  $g_{3/2}/g_{1/2} = 2$ . If we adopt column densities which result from using the maximum value of the stellar background level the ratio,  $N'(C_{3/2}^+)/N'(C_{1/2}^+)$ , becomes 1.5 reflecting principally on the decreasing importance of corrections. This fact illustrates how critical the estimate of the  $C^+$  ion column density outside the cloud is - both in the case of  $\zeta$  Oph and in other cases where the Stromgren sphere contains significant amounts of material. It should be noted, in this respect, that another way of reducing the  $N(C_{3/2}^+)/N(C_{1/2}^+)$  ratio is by changing the interstellar gas model so that the H I region with  $n(H) = 0.07 \text{ cm}^{-3}$  extends all the way from the ionization front to the earth excepting the cloud itself. In this case the population ratio is 1.4, again the importance of the corrections to the  $N(C_{1/2}^+)$  column density is demonstrated.

Since the excitation or de-excitation rates are simply the product of the hydrogen atom density and the collision rates per hydrogen atom equation (7) may be used to calculate  $n(H)$ . Using a value for  $w(3/2, 1/2)$  of  $2.36 \times 10^{-6} \text{ sec}^{-1}$  (Bahcall and Wolf, 1968) and the collision rates listed in Table 4 it is found for a population ratio of 1.5 that there is no hydrogen atom density sufficiently large to produce the required population of the  $2p_{3/2}$  level at any of the temperatures included in Table 4. If the population ratio is reduced somewhat

arbitrarily to 1.0 then the derived hydrogen atom density becomes  $3.3 \times 10^4 \text{ cm}^{-3}$  at  $150^\circ\text{K}$ ,  $1.2 \times 10^4 \text{ cm}^{-3}$  at  $200^\circ\text{K}$ , and  $0.82 \times 10^4 \text{ cm}^{-3}$  at  $250^\circ\text{K}$ .

While uncertainties remain in the corrections to the  $\text{C}_{1/2}^+$  column density and in the collision cross-sections the hydrogen atom densities derived above are probably minimum values. As such, they are considerably larger than the density of  $730 \text{ cm}^{-3}$  found by Herbig (1968) for the same interstellar gas model as is employed in this paper. There is an additional problem concerning the implied electron density within the cloud. Using the assumed ratio of the electron density to the hydrogen atom density of  $6 \times 10^{-4}$  and a hydrogen atom density of  $10^4$ , the implied electron density is  $6 \text{ cm}^{-3}$ . On the other hand, Herbig (1968) gives an upper limit on the electron density of  $1.9 \text{ cm}^{-3}$  which is based on the measured line strengths of the Ca II (3933.7, 3968.5Å) doublet and the absence of the Ca I (4226.7Å) line. More recently, Bortolot, Shulman, and Thaddeus (1972) have established on the basis of the calcium lines that the electron density lies between 0.06 and  $0.4 \text{ cm}^{-3}$ .

Corroborative evidence for cloud densities appreciably less than  $10^4 \text{ cm}^{-3}$  comes from the CO bands of the fourth positive system found in the  $\zeta$  Oph spectrum (Smith and Stecher, 1971). Although it was impossible in this work to resolve line structure within a band, the band strengths were large enough to indicate that each band was comprised of several lines. In fact, the

results were consistent with the supposition that the first three levels of the ground state were populated by cosmic blackbody radiation. When a curve of growth was computed assuming that the molecules were in thermodynamic equilibrium with an ambient gas at  $20^{\circ}\text{K}$  a satisfactory fit of the data points to the curve of growth produced a turbulence parameter equal to  $0.47 \text{ km sec}^{-1}$ . The lowest value of the turbulence parameter determined by Herbig (1968) was  $0.85 \text{ km sec}^{-1}$  and was based on the  $\text{CH}^+$  molecular spectrum. Thus, it is not likely that the CO molecules are in thermodynamic equilibrium with a gas of temperature equal to or greater than  $20^{\circ}\text{K}$ , but this condition would certainly exist if the cloud density was  $10^4 \text{ cm}^{-3}$ .

A possible alternative to collisional excitation of the  $^2\text{P}_{3/2}^{\text{O}}$  level in  $\text{C}^+$  ions is to suppose that coherent scattering of  $1334.5\text{\AA}$  quanta within the interstellar cloud populates the upper  $^2\text{D}_{3/2}$  level at a rate sufficiently high that subsequent decays to the  $^2\text{P}_{3/2}^{\text{O}}$  level produce the observed ground state fine structure level population ratio. The expression giving the absorption rate per ion is simply  $B(\nu)F(\nu)$  where  $B(\nu)$  is the Einstein absorption coefficient and  $F(\nu)$  is the stellar flux in units of  $\text{ergs cm}^{-2} \text{ sec}^{-1} (\text{cps})^{-1}$ . Assuming the cloud to be 15 pc from the star, and using the flux measurements of Smith (1967) for  $\zeta \text{ Oph}$  at  $1376\text{\AA}$  the stellar flux entering the cloud is estimated to be  $2.54 \times 10^{-18} \text{ ergs cm}^{-2} \text{ sec}^{-1} (\text{cps})^{-1}$ , a value which includes a correction made for interstellar

reddening. As an estimate of the effect of scattering, the flux is increased in the cloud by a factor of  $\tau_0^2$  where  $\tau_0$  is the optical depth in the center of the C II (1334.7Å) line. The factor  $\tau_0^2$  gives the order of the number of scatterings before a  $\lambda 1334.7\text{\AA}$  photon escapes assuming a 100% albedo from grains in the cloud and no redistribution of photon frequencies during collisions. The optical depth in question is 5.0,  $\tau_0^2$  is 25, and thus  $F(\nu)$  becomes  $6.35 \times 10^{-17} \text{ ergs cm}^{-2} \text{ sec}^{-1} (\text{cps})^{-1}$ . The absorption rate per ion is then  $2.97 \times 10^{-7} \text{ sec}^{-1}$ . The probability that a  $\text{C}^+$  ion excited to the  $^2\text{D}_{3/2}$  level will decay to the  $^2\text{P}_{3/2}^0$  level is 0.172, and consequently the estimated rate of population of the  $^2\text{P}_{3/2}^0$  level in this way is  $0.0503 \times 10^{-6} \text{ sec}^{-1}$ . The de-population of the  $^2\text{P}_{3/2}^0$  level by the reverse process is about 1/2 the population rate. When the population rate is compared to the radiative decay rate of  $2.36 \times 10^{-6} \text{ sec}^{-1}$  (Bahcall and Wolf, 1968) it is apparent that this population mechanism cannot work. Furthermore, a more accurate treatment can only reduce the population rate.

Thus, it becomes evident that the easiest way to resolve the discrepancies implicit in the assumption that most of the detected interstellar material is in one cloud is to suppose that a large part of the C II spectrum arises outside the strong,  $-15 \text{ km sec}^{-1}$  cloud. The fact that unacceptably high densities are required by the observations if the  $\text{C}^+$  ions are located in an H I region suggests that the extra  $\text{C}^+$  ions are located within

the Strömgren sphere. If the hydrogen of the "interior" cloud is assumed to be completely ionized and at a temperature of  $10^4$  K then the density required to produce the relative ground state level populations in  $C^+$  may be calculated. The electron collision cross-sections are given by equation (8), and the proton collision cross-sections may be estimated from a graphical representation of  $\langle\sigma v\rangle$  vs.  $T$  given on page 715 of Bahcall and Wolf (1968). Assuming, as before, that the population ratio of the  $2P_{3/2}^0$  to  $2P_{1/2}^0$  level in  $C^+$  is 1.5 then the density of electrons or protons necessary to produce this ratio is  $220 \text{ cm}^{-3}$ , a not unreasonable value.

The question arises as to why the comparable  $2P_{3/2}^0$  level at 0.036 eV in  $Si^+$  ions is not also populated to an observable degree. The answer is that the radiative decay rate between the fine structure levels is comparatively large, i.e.  $2.13 \times 10^{-4} \text{ sec}^{-1}$  (Bahcall and Wolf, 1968). This figure together with the proton collision cross-section, again estimated from Bahcall and Wolf (1968), and the density of  $220 \text{ cm}^{-3}$  derived from the C II lines combine to give a population ratio of  $3.4 \times 10^{-3}$ . The electron collision cross-sections are small compared to the proton cross-sections, and may be neglected. Thus, one should not expect to see excitation of the  $2P_{3/2}^0$  level in  $Si^+$  ions at densities on the order of  $220 \text{ cm}^{-3}$ .

For the case of the  $3P_1$  fine structure level in oxygen atoms an upper limit to the proton collision de-excitation cross-section is given by equation (31d) of Bahcall and Wolf (1968)

reproduced here as

$$\langle \sigma(J = 1 \text{ to } J = 2)v \rangle = (2.5 \times 10^{-8} \text{ cm}^3 \text{ sec}^{-1}) \langle r^2 \rangle \quad (9)$$

where  $\langle r^2 \rangle$  is the mean square radius of the atom's outer shell of electrons in units of  $\text{\AA}^2$ , and in this case takes on the value of 0.55. Multiplying equation (9) by  $g_1/g_0 \exp(-\chi/kT) = 2.93$  to obtain the excitation cross-section, using a density of  $220 \text{ cm}^{-3}$  and a radiative decay rate between the  $^3P_1$  and  $^3P_2$  fine structure levels of  $8.95 \times 10^{-5} \text{ sec}^{-1}$  (Bahcall and Wolf, 1968) an upper limit to the population ratio of these fine structure levels is 0.10. Thus, the longward side of the spectral feature centered on  $\lambda 1304.4 \text{\AA}$  and due mainly to the Si II ( $1304.4 \text{\AA}$ ) line may reflect the population of the  $^3P_1$  level in oxygen atoms located inside the Strömgren sphere.

In exactly the same way as outlined above it can be shown that the relative population of the  $^3P_2$  level (0.0163 eV) to the  $^3P_0$  ground level in  $N^+$  ions is 0.044. Thus one can expect to find an interstellar feature at  $\lambda 1084 \text{\AA}$  composed of a resonance line, N II ( $1084.0 \text{\AA}$ ), and two lines arising from the  $^3P_2$  level, N II ( $1085.7, 1085.5 \text{\AA}$ ). The population of the third fine structure level,  $^3P_1$ , should be about a factor of 4.3 smaller than the  $^3P_2$  level. Unfortunately, this region of the spectrum was not recorded due to a payload malfunction. Such an observation would provide useful evidence bearing on the hypothesis of collisional excitation of some interstellar atoms and ions.

Assuming that the population ratio of the ground state

fine structure levels is 1.5 the column density of  $C^+$  ions inside the Strömgren sphere is  $1.67 \times 10^{17} \text{ cm}^{-2}$ . This result also depends on the assumption that all of the C II (1335.7Å) line arises in the Strömgren sphere. The column density of sodium in both atomic and singly ionized form is  $1.33 \times 10^{15} \text{ cm}^{-2}$  assuming solar abundances. If the material is located 4 pc from the star the photoionization and recombination coefficients for atomic sodium may be obtained from Herbig (1968), page 255, Table 5, and these values together with an electron density of  $220 \text{ cm}^{-3}$  may be put in equation (4) to obtain the ratio of  $n(\text{Na}^+)/n(\text{Na}^0)$  which is equal to 132. Therefore, the column density of sodium atoms in the Stromgren sphere becomes  $1.0 \times 10^{-13} \text{ cm}^{-2}$  which is approximately 1/5 of the sodium atom column density observed by Herbig (1968). Since in any case, the contribution to the observed  $\text{Na}^0$  column density from regions outside concentrations of interstellar material is small the hypothesis put forward here that there is some material with density equal to  $220 \text{ cm}^{-3}$  within the Strömgren sphere is not basically inconsistent with the visible observations.

## VII. MASS LOSS FROM $\zeta$ OPH

It is possible that the hypothetical interior cloud is simply an ordinary H I interstellar cloud which was overtaken by the ionization front surrounding  $\zeta$  Oph. Another possibility is that the interior cloud is formed by matter escaping from  $\zeta$  Oph itself, and the evidence for this conjecture is now discussed.

In Figure 4a, b are shown two portions of the  $\zeta$  Oph spectrum containing evidence for what is interpreted to be stellar material moving radially outward from the star. Figure 4a shows two strong features at 1233.2 and 1237.3 $\text{\AA}$  which are correlated with the N V resonance lines at the laboratory wavelengths 1238.8 and 1242.8 $\text{\AA}$  respectively. A relatively weak feature at 1240.5 $\text{\AA}$  has been tentatively associated with Mg II (1239.9, 1240.4 $\text{\AA}$ ) resonance transitions and Al IV (1240.2, 1240.8 $\text{\AA}$ ) subordinate transitions. There is an Al IV (1237.1 $\text{\AA}$ ) line which lies close to the 1237.3 $\text{\AA}$  feature, but throughout the entire recorded spectral range there is no evidence that the Al IV spectrum is strong. It is, therefore, unlikely that the Al IV (1237.1 $\text{\AA}$ ) line can account for such a strong feature.

Figure 4b shows a similar situation prevailing for C<sup>+++</sup> ions. The minima of the large absorption feature located at 1541.8 and 1544.5 $\text{\AA}$  are correlated with the laboratory measured resonance lines at 1548.2 and 1550.8 $\text{\AA}$  respectively. It appears that the shape of the spectrum contour between 1545 and 1556 $\text{\AA}$  indicates that there is emission associated with this feature as well as absorption. The feature has been noted and reported previously (Smith and Stecher, 1971). As is shown in this

reference the (0,0) vibrational transition of the fourth positive system in the CO spectrum would be seen if there were sufficient background continuum radiation at  $1544\overset{\circ}{\text{\AA}}$ . However, based on the strengths of the bands appearing in the CO spectrum this feature would be weak. In addition, there are subordinate Cl IV lines at 1545.2, 1549.2 and  $1551.3\overset{\circ}{\text{\AA}}$  which are also expected to be weak.

Finally, in Figure 4c are shown the strong features associated with the Si IV ( $1393.7, 1402.7\overset{\circ}{\text{\AA}}$ ) resonance lines. The minima of these features occur very nearly at the laboratory wavelengths, and there is some small asymmetry to the features which exhibit more absorption on the shortward side of the minima. There are, however, no large shortward shifted absorption features associated with these lines. Another CO line corresponding to the (5,0) band in the fourth positive system measurably affects the short wavelength side of the Si IV ( $1393.7\overset{\circ}{\text{\AA}}$ ) line, but the strength of the molecular band is much less than the strength of the Si IV line.

The standard interpretation of Figures 4a and 4b, and that which is adopted here, is that the  $\text{C}^{+++}$  and  $\text{N}^{++++}$  ions are accelerated by momentum transfer from the radiation field (Lucy and Solomon, 1967). The fact that the  $\text{Si}^{+++}$  ions do not seem to share this radial motion can be explained if one assumes that at altitudes where the momentum transfer occurs most silicon is more highly ionized, i.e. in the form of  $\text{Si}^{++++}$ , and the  $\text{Si}^{+++}$  ions are at lower levels where the atmosphere has not achieved any observable outward velocity. With this in mind

one might also expect to observe the resonance lines of O VI (1031.9, 1037.6 $\text{\AA}$ ) shifted to shorter wavelengths if the wavelength coverage could be extended down to the region of LB at 1025.7 $\text{\AA}$ . Certainly, such an interpretation is extraordinary for a star whose classification is O9.5V, but it is nevertheless considered the simplest explanation of the observations.

One can easily calculate the average radial velocities of the  $\text{C}^{+++}$  and  $\text{N}^{++++}$  ions corresponding to the minima of the shortward shifted absorption features; these are 1340 and 1230 km sec $^{-1}$  respectively. Both of these values exceed the escape velocity from the star of 901 km sec $^{-1}$  calculated under the assumptions that the mass of  $\zeta$  Oph is  $17 M_{\odot}$  and the radius is  $8R_{\odot}$ . The ions, however, are slowed down in their outward flight by coulomb forces exerted on them principally by the protons in the H II region. At a temperature of  $10^4$  (K) the protons have a mean velocity of about  $10^6$  cm sec $^{-1}$  which is at least two orders of magnitude less than the  $\text{C}^{+++}$  ions. Following Spitzer (1967, 1968) a slowing down time,  $t_s$ , can be defined so that the average change of velocity per collision is  $w/t_s$  where  $w$  is the initial ion velocity. The expression relating  $t_s$  to the initial velocity is

$$t_s = \frac{2w^3}{\left(1 + \frac{m}{m_f}\right) A_D} \quad (10)$$

where  $m$  and  $m_f$  are the masses of the ion and field particle, i.e. proton, respectively. The diffusion constant  $A_D$  is

$$A_D = \frac{8\pi e^4 n_f Z_f^2 \ln \Lambda}{m^2} \quad (11)$$

where  $n_f$  is the density of field particles or  $3 \text{ cm}^{-3}$ ,  $\frac{Ze}{c}$  and  $\frac{Z_f e}{c}$  are the electrical charges of the ions and field particles in emu units respectively, and  $\ln \Lambda$  is a "cut-off" factor which accounts for the fact that beyond a limited range the coulomb forces are ineffective. In the case at hand  $\ln \Lambda$  is about 22. Application of equations (10) and (11) show that for the  $C^{+++}$  and  $N^{++++}$  ions the slowing down time is  $1.89 \times 10^{11}$  sec and  $1.63 \times 10^{11}$  sec respectively. If an average stopping distance,  $\bar{I}$ , is defined by the relation  $\bar{I} = (w/2)t_s$  then for the  $C^{+++}$  and  $N^{++++}$  ions  $\bar{I}$  equals 4.1 and 3.2 pc respectively. The suggestion is made that the material leaving the star slows down and stops in the gas of the H II region at distances up to 4 pc where the ions assume a distribution among ion states determined by the ionization coefficient,  $\Gamma$ , and the recombination coefficient,  $\alpha$ , characteristic of the radiation field and electron density at these distances. If the electron density were  $220 \text{ cm}^{-3}$  and the temperature  $10^4 \text{ (K)}$  the predominant ionic states would be  $C^+$ ,  $N^+$ ,  $O^+$ ,  $P^+$ , and  $S^+$ . In this picture a low density annulus is built up at large distances from the star which probably shares the expansion velocity of the surrounding gas in the H II region. The extent of the absorbing region along the line of sight may be easily estimated if it is assumed that the population ratio of the  $2P_{3/2}^o$  to  $2P_{1/2}^o$  levels in  $C^+$  is 1.5, that all of the  $C^+$  in the  $2P_{3/2}^o$  state is inside the Strömberg sphere, that the proton density is  $220 \text{ cm}^{-3}$ , and that solar abundances apply.

The answer is that the line-of-sight dimension of the absorbing region is 0.47 pc.

## VIII. ABUNDANCES

As discussed in Section IV the derived column densities of carbon atoms and  $S^+$  ions are quite uncertain due primarily to inadequate instrumental resolution. Estimates of the column density of  $C^+$  and  $Si^+$  ions and oxygen atoms can be made, however, and compared to the column density of hydrogen determined from the  $L\alpha$  line. To do this it is necessary to subtract from the measured column densities the estimated contributions from the H II region. These are composed of two parts, one, an ionized gas with  $n(e)$  equal to  $3\text{ cm}^{-3}$ , and the other, an ionized gas with  $n(e)$  equal to  $220\text{ cm}^{-3}$ . The contribution of the first part may be obtained from Table 3. The contribution of the second part can be estimated if, as before, all the  $C^+$  ions in the  $2p_{3/2}^o$  state are assumed to be inside the Strömgren sphere and that the population ratio of the  $2p_{3/2}^o$  level to the  $2p_{1/2}^o$  level is 1.5. Turning to Table 1 for the column density of  $C^+$  ions in the  $2p_{3/2}^o$  level it is found that the number of  $C^+$  ions in the  $2p_{1/2}^o$  level contained by the interior cloud is  $0.93 \times 10^{17}\text{ cm}^{-2}$  if the largest value permitted by the uncertainty in locating the background continuum is used. This value is appropriate for use in conjunction with the 1.5 population ratio.

To estimate the contribution from the interior cloud to the  $Si^+$  ion and oxygen atom column densities the total column density of  $C^+$  ions,  $1.93 \times 10^{17}\text{ cm}^{-2}$ , was used together with solar abundance ratios. In the case of oxygen atoms the column

density derived in this way was reduced by an additional factor of 0.1 to allow for the population of the  $^3P_1$  level as discussed in Section V. No correction for a possible contribution to the O I (1302.2 $\text{\AA}$ ) line from telluric oxygen atoms was made since the standard atmosphere estimate discussed in Section IV was negligibly small, and the excitation of the O I (1304.9 $\text{\AA}$ ) line has been assumed due exclusively to collisions occurring inside the Strömgren sphere.

The results are given in Table 5. The identity of the atom or ion and the line from which the column densities are determined are listed in columns 1 and 2 respectively. The column densities corrected for contributions from the H II region appear in column 3. The ratio of the corrected column density to the measured column density of hydrogen ( $4.6 \times 10^{20} \text{ cm}^{-2}$ ) is listed in column 4, and the solar abundance ratio is listed in column 5. Again, the uncertainties appearing in column 3 are due only to the uncertainty in locating the background stellar continuum level. The  $\text{Si}^+$  ion abundance ratio results from averaging the corrected column densities determined from both the Si II (1304.4 $\text{\AA}$ ) and the Si II (1526.7 $\text{\AA}$ ) lines. The column density associated with the Si II (1260.4 $\text{\AA}$ ) line became negative when the correction was applied, and therefore, was not used. This absurdity means that the inaccuracies of both the measurement and the correction procedures are too large to enable one to derive a significant abundance ratio from the Si II (1260.4 $\text{\AA}$ ) line. Unfortunately, the same lack of

precision affects the abundance ratios determined from the other lines; it is, perhaps, surprising that the agreement with solar abundance ratios is as good as it is. All that can be said is that the present results give no reason to believe that the interstellar abundances of carbon, oxygen, and silicon depart radically from solar abundances of these elements.

The question arises as to whether contributions from within the Stromgren sphere could account for the anomalously large equivalent widths of the interstellar C I and S II lines. A glance at Table 3 will show that in the case of the carbon atoms such a contribution would have to come from the postulated interior cloud since the column density through regions where  $n(e) = 3 \text{ cm}^{-3}$  is expected to be only  $3.2 \times 10^{13} \text{ cm}^{-2}$ . Assuming that in the interior cloud the column density of  $C^+$  ions is  $1.93 \times 10^{17} \text{ cm}^{-2}$ ,  $n(e) = 220 \text{ cm}^{-3}$ , and that  $\Gamma/\alpha = 2.5 \times 10^4$  (see Table 2) it is easily seen by using equation (4) that the columnar density of carbon atoms is  $1.7 \times 10^{15} \text{ cm}^{-2}$ . This column density corresponds to  $\log \tau_0 \approx 2$ , and referring to Figure 3 it can be seen that the corresponding value of  $\log (W_\lambda/b_\lambda)$  is almost included within the error estimates of the observation when the single-cloud curve of growth is used. If the carbon atoms were located in the postulated interior cloud and in one or more clouds outside the H II region there would be no difficulty at all in reconciling the observed equivalent widths of the carbon lines with reasonably small ( $\approx 2 \times 10^5 \text{ cm}^{-2}$ ) carbon atom column densities.

The situation for the  $S^+$  ions is not so clear. Assuming that solar abundances prevail the total column density of  $S^+$  ions within the Stromgren sphere is estimated to be  $1.0 \times 10^{16} \text{ cm}^{-2}$ . This figure is at least a factor of 10 smaller than the observed  $S^+$  ion column density even when observational errors have been assumed to exist. Therefore, it is necessary to postulate that the absorption features attributed to  $S^+$  ions must to a large extent arise in regions outside the H II region which itself makes a relatively minor contribution..

Finally, it is possible to compare the corrected column densities of  $C^+$  ions and oxygen atoms listed in Table 5 with the CO molecule column density of  $1.8 \times 10^{15} \text{ cm}^{-2}$  previously measured by Smith and Stecher (1971). The result is that along the line-of sight and outside the Stromgren sphere approximately 4% of the interstellar carbon and 0.1% of the interstellar oxygen is in the form of CO molecules.

## IX. SUMMARY

Presented in this paper are observations of interstellar lines arising in  $C^0$ ,  $C^+$ ,  $O^0$ ,  $Si^+$ , and  $S^+$  found in the ultraviolet spectrum of  $\zeta$  Oph. In addition, the stellar absorption lines of C IV (1548.2, 1550.8Å), N V (1238.8, 1242.8Å), and Si IV (1393.8, 1402.8Å) are reproduced, the first two of which are shifted to shorter wavelengths by about 6Å. Determinations of interstellar column densities have been combined with a model for the distribution of intercloud material with the following results.

1. The abundance ratios obtained by dividing the  $C^+$ ,  $O^0$ , and  $Si^+$  column densities extending from the boundary of the Strömberg sphere to the sun by the hydrogen atom column density are consistent with the corresponding solar abundance ratios, the agreement being within a factor of 10. The results imply that the  $C^0$  and  $S^+$  atoms and ions are distributed among several clouds, and if there is no stratification of the species represented here the  $C^+$ ,  $O^0$ , and  $Si^+$  atoms and ions are similarly distributed. Lines arising in the latter group lie on the square root portion of the curve of growth and are relatively insensitive to the distribution of these particles. Such is not the case for the  $C^0$  lines which are probably unresolved blends of closely spaced multiplet members which lie on or near the flat portion of the curve of growth. The column density of C atoms is in this case very sensitive to the distribution of atoms in the line-of-sight.

2. The  $^2P_{3/2}^o$  (0.0079 eV) level in  $C^+$  ions is strongly populated. If the maximum column densities permitted by uncertainties in the background stellar flux are used the population ratio of the  $^2P_{3/2}^o$  level to the  $^2P_{1/2}^o$  level is 1.5. It is suggested that the excited  $C^+$  ions are located inside the Strömgren sphere where proton densities equal to or greater than  $220 \text{ cm}^{-3}$  would permit the  $^2P_{3/2}^o$  level to be populated by collisions.
3. The shortward shifted absorption lines of C IV (1548.2, 1550.8Å) and N V (1238.8, 1242.8Å) indicate that matter is escaping from  $\zeta$  Oph. However, the coulomb forces between the escaping matter and the residual protons inside the Strömgren sphere will stop the stellar matter well short of the ionization front, indeed, probably within a distance less than 4 pc from the star. The suggestion is made that upon recombination in the H II region, part of the escaping  $C^{+++}$  ions become  $C^+$  ions in the  $^2P_{3/2}^o$  state, and thus contribute to the large population observed for this level.

## ACKNOWLEDGEMENTS

I wish to thank Messrs. A. K. Stober, G. R. Baker, and R. Scolnik for their great assistance both in preparing the instrument and in the launch and recovery operations. Also, special thanks go to Mrs. Jan Niebur and Miss Susan Brewer for their assistance with the calculations and to Dr. Anne B. Underhill for helpful and stimulating discussions.

TABLE 1

EQUIVALENT WIDTHS AND DERIVED COLUMN DENSITIES OF  
LINE IN THE INTERSTELLAR SPECTRUM OF  $\zeta$  OPH

Line Identification	$W_{\lambda}$ ( $\text{\AA}$ )	1 Cloud ( $\text{cm}^{-2}$ )	2 Cloud ( $\text{cm}^{-2}$ )
C I (1277.25 $\text{\AA}$ )	$0.241 \pm 0.094$	$(1.5^{+4.8}_{-1.3}) 10^{17}$	$(3.6^{+21.5}_{-2.7}) 10^{15}$
C I (1328.83 $\text{\AA}$ )	$0.195 \pm 0.064$	$(6.2^{+6.4}_{-4.2}) 10^{17}$	$(3.2^{+21.4}_{-2.8}) 10^{16}$
C II (1334.53 $\text{\AA}$ )	$0.254 \pm 0.037$	$(1.4^{+0.5}_{-0.3}) 10^{17}$	$(1.2^{+0.4}_{-0.4}) 10^{17}$
C II (1335.68 $\text{\AA}$ )	$0.235 \pm 0.039$	$(1.0^{+0.4}_{-0.3}) 10^{17}$	$(0.68^{+0.35}_{-0.28}) 10^{17}$
O I (1302.17 $\text{\AA}$ )	$0.262 \pm 0.046$	$(2.2^{+0.9}_{-0.6}) 10^{18}$	$(1.7^{+1.0}_{-0.6}) 10^{18}$
Si II (1260.42 $\text{\AA}$ )	$0.281 \pm 0.047$	$(0.87^{+0.45}_{-0.24}) 10^{16}$	$(0.79^{+0.39}_{-0.23}) 10^{16}$
Si II (1304.37 $\text{\AA}$ )	$0.130 \pm 0.045$	$(6.5^{+5.5}_{-3.1}) 10^{16}$	$(3.7^{+5.0}_{-2.2}) 10^{16}$
Si II (1526.72 $\text{\AA}$ )	$0.195 \pm 0.057$	$(6.8^{+2.1}_{-3.6}) 10^{16}$	$(3.8^{+3.3}_{-1.8}) 10^{16}$
S II (1250.50 $\text{\AA}$ )	$0.156 \pm 0.040$	$(4.3^{+2.5}_{-1.9}) 10^{19}$	$(2.6^{+3.7}_{-1.7}) 10^{19}$
S II (1253.79 $\text{\AA}$ )	$0.167 \pm 0.048$	$(2.9^{+1.9}_{-1.4}) 10^{19}$	$(1.9^{+4.1}_{-1.9}) 10^{19}$
S II (1259.53 $\text{\AA}$ )	$0.118 \pm 0.037$	$(1.4^{+1.1}_{-0.8}) 10^{19}$	$(6.6^{+16.8}_{-5.7}) 10^{18}$

TABLE 2  
PHOTOIONIZATION COEFFICIENTS,  $\Gamma$ , AND RECOMBINATION COEFFICIENTS,  
 $\alpha$ , FOR VARIOUS DISTANCES FROM  $\zeta$  OPH

$x$ (pc)	$C^0$	$C^+$	$Si^0$	$Si^+$	$O^0$	$O^+$
2	3.17 (-8)	3.21 (-12)	2.80 (-7)	7.96 (-11)	7.26 (-10)	1.30 (-11)
4	8.18 (-9)	8.03 (-13)	7.15 (-8)	1.99 (-11)	1.81 (-10)	3.25 (-12)
6	3.82 (-9)	3.57 (-13)	3.29 (-8)	8.85 (-12)	8.06 (-11)	1.44 (-12)
10	1.59 (-9)	1.28 (-13)	1.31 (-8)	3.19 (-12)	2.90 (-11)	5.20 (-13)
15	7.90 (-10)	5.71 (-14)	6.91 (-9)	1.41 (-12)	1.29 (-11)	2.31 (-13)
$\alpha(T = 10^{40}K)$	0.33 (-12)	6.23 (-12)	0.41 (-12)	0.41 (-12)	0.22 (-12)	0.41 (-12)
15	7.49 (-10)	0.00	6.89 (-9)	0.00	0.00	0.00
20	5.23 (-10)	0.00	4.74 (-9)	0.00	0.00	0.00
50	2.78 (-10)	0.00	2.41 (-9)	0.00	0.00	0.00
170	2.36 (-10)	0.00	2.00 (-9)	0.00	0.00	0.00
$\alpha(T = 10^{20}K)$	7.6 (-12)		8.6 (-12)			

TABLE 3

COLUMN DENSITIES BETWEEN THE BOUNDARIES OF THE  
MODEL INTERCLOUD GAS DISTRIBUTION

Region Thick- ness (pc)	$N(H^0)$ ( $cm^{-2}$ )	$N(C^0)$ ( $cm^{-2}$ )	$N(C^+)$ ( $cm^{-2}$ )	$N(Si^0)$ ( $cm^{-2}$ )	$N(Si^+)$ ( $cm^{-2}$ )	$N(O^0)$ ( $cm^{-2}$ )	$N(O^+)$ ( $cm^{-2}$ )
0-15	0.00	3.20 (+13)	5.46 (+16)	8.73 (+10)	8.55 (+14)	2.12 (+15)	1.18 (+17)
15-20	4.63 (+19)	5.37 (+11)	2.41 (+16)	4.10 (+9)	1.48 (+15)	4.21 (+16)	0.00
20-170	3.24 (+19)	2.95 (+10)	1.69 (+16)	2.40 (+8)	1.04 (+15)	2.95 (+16)	0.00

TABLE 4

COLLISION RATES PER HYDROGEN ATOM FOR TRANSITIONS BETWEEN THE  
GROUND STATE FINE STRUCTURE LEVELS OF C<sup>+</sup>

Temperature (°K)	J-J'	$\langle\sigma v\rangle$ (cm <sup>3</sup> sec <sup>-1</sup> )	
		Electrons	Hydrogen Atoms
100	$\frac{1}{2} - \frac{3}{2}$	1.50(-10)	5.41(-10)
	$\frac{3}{2} - \frac{1}{2}$	1.86(-10)	6.74(-10)
150	$\frac{1}{2} - \frac{3}{2}$	1.66(-10)	7.01(-10)
	$\frac{3}{2} - \frac{1}{2}$	1.52(-10)	6.44(-10)
200	$\frac{1}{2} - \frac{3}{2}$	1.67(-10)	8.05(-10)
	$\frac{3}{2} - \frac{1}{2}$	1.32(-10)	6.35(-10)
250	$\frac{1}{2} - \frac{3}{2}$	1.64(-10)	8.60(-10)
	$\frac{3}{2} - \frac{1}{2}$	1.18(-10)	6.19(-10)

TABLE 5

ABUNDANCE RATIOS DETERMINED FROM THE INTERSTELLAR  
SPECTRUM OF  $\zeta$  OPH

Ion or Atom	Absorption Line( $\text{\AA}$ )	Corrected Column Density ( $\text{cm}^{-2}$ )	Abundance Ratio	Solar Abundance Ratio
$\text{C}^+$	1234.5	$0.4 \times 10^{17}$	$0.9 \times 10^{-4}$	$5.2 \times 10^{-4}$
$\text{O}^0$	1302.2	$(1.9^{+0.9}_{-0.6}) 10^{18}$	$41 \times 10^{-4}$	$9.1 \times 10^{-4}$
$\text{Si}^+$	1304.4	$(5.2^{+5.5}_{-3.1}) 10^{16}$	$12 \times 10^{-5}$	$3.2 \times 10^{-5}$
$\text{Si}^+$	1526.7	$(5.5^{+2.1}_{-3.6}) 10^{16}$		

# REFERENCES

- Bahcall, J. N., and Wolf, R. A. 1968, Ap. J., 152, 701.
- Sortolot, V. J., Shulman, S., and Thaddeus, P. 1972, to be published in the Ap. J.
- Bradley, P. T., and Morton, D. C. 1969, Ap. J., 156, 687.
- Chapman, R. D., and Henry, R. W. J. 1972 to be published in the Ap. J., 173.
- Field, G. B., and Hitchcock, J. L. 1966, Ap. J., 146, 1.
- Goldberg, L., Muller, E. A., and Aller, L. H. 1960, Ap. J. Suppl., 5, 1.
- Habing, H. J. 1968, Bull. Astr. Inst. Netherlands, 19, 421.
- Herbig, G. H. 1968, Z.f. Astrophys., 68, 243.
- Jenkins, E. B. 1969, in "Ultraviolet Stellar Spectra and Related Ground-Based Observations" (International Astronomical Union Symposium No. 36) eds. L. Houziaux and H. E. Butler (Dordrecht: D. Reidel Publishing Company).
- Lucy, L. B., and Solomon, P. M. 1967, A. J., 72, 310.
- Penston, M. V. 1970, Ap. J., 162, 771.
- Seaton, M. J. 1951, M. N., 111, 368.
- \_\_\_\_\_. 1958, Rev. Mod. Phys., 30, 979.
- Silk, J., and Brown, R. L. 1971, Ap. J., 163, 495.
- Slettebak, A., 1956, Ap. J., 124, 173.
- Smith, A. M. 1970, Ap. J., 160, 595.
- Smith, A. M., and Stecher, T. P. 1971, Ap. J., 164, 143.
- Spitzer, L. 1967, "Physics of Fully Ionized Gases" (New York: John Wiley & Sons).
- \_\_\_\_\_. 1968, "Diffuse Matter in Space" (New York: John Wiley & Son)
- Stone, M. E., and Morton, D. C. 1967, Ap. J., 149, 29.
- Stromgren, B. 1948, Ap. J., 108, 212.

U. S. Standard Atmosphere Supplements, 1966 (Washington: U.S. Government Printing Office).

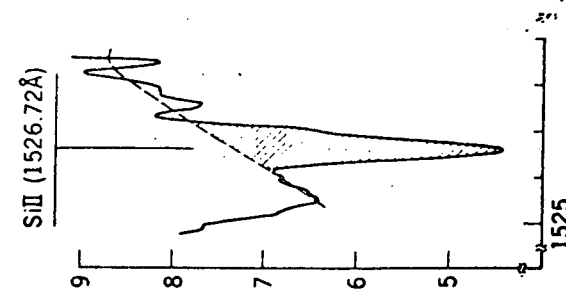
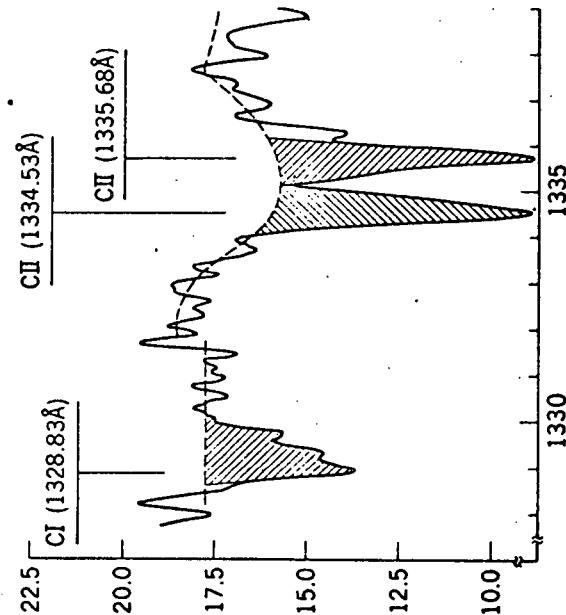
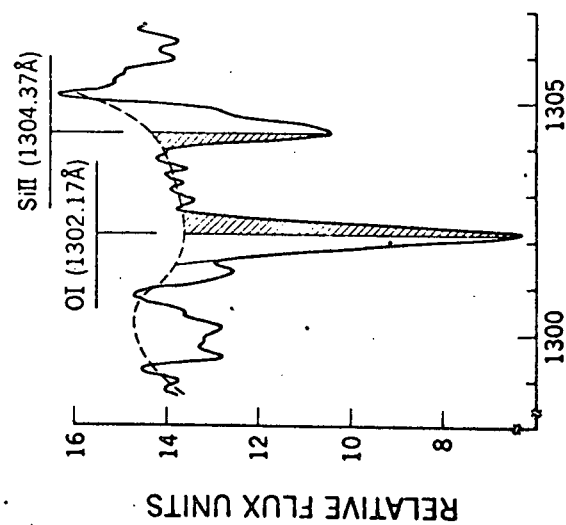
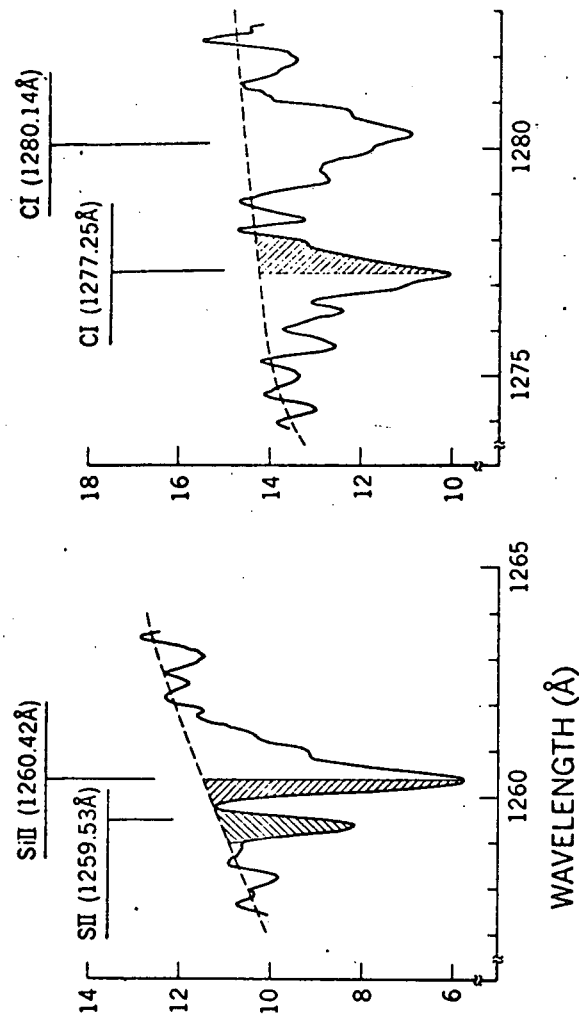
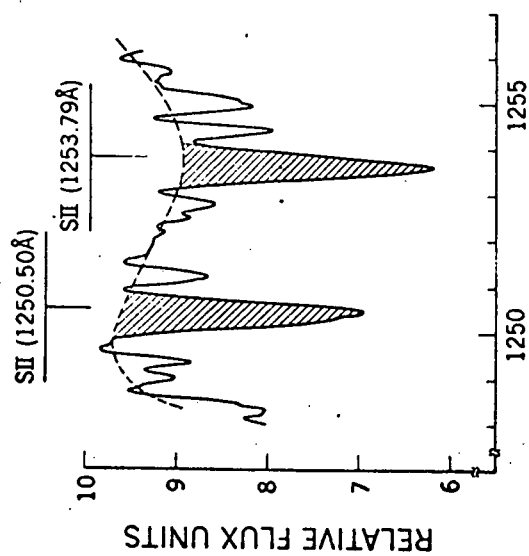
Weisheit, J. C., and Lane, N. F. 1971, Phys. Rev. A, 4, 171.

Wiese, W. L., Smith, M. W., and Glennon, B. M. 1966, NSRDS-NBS4, 1, 1.

Wiese, W. L., Smith, M. W., and Miles, B. M. 1969, NSRDS-NBS 22, 2, 1.

## FIGURE CAPTIONS

- Fig. 1 - Segments of the  $\zeta$  Oph spectrum containing various interstellar lines. Abscissae, wavelengths in Angstrom units. Ordinates, flux in relative units. Dashed lines indicate the assumed background stellar flux, cross-hatching the area used in computing equivalent widths.
- Fig. 2 - Rectified flux distribution of the  $\text{La}$  line. Abscissae, wavelength in Angstrom units. Ordinates, flux in relative units. Features due to  $\text{N}^{\text{O}}$ ,  $\text{Si}^{++}$ , and  $\text{H}_2\text{O}$  which modify the  $\text{La}$  line contour are indicated. Dashed curve is a computed profile fitted to the core of the observed line.
- Fig. 3 - Curves of growth for the C I ( $1277.2\text{\AA}$ ) and C II ( $1334.5\text{\AA}$ ) lines computed assuming that interstellar matter is distributed in one cloud or two clouds. Abscissae, log of the optical depth in the center of the line. Ordinates, log of the line equivalent width divided by the Doppler width.
- Fig. 4 - Segments of the  $\zeta$  Oph spectrum containing the stellar lines of (a) N V ( $1238.8$ ,  $1242.8\text{\AA}$ ), (b) C IV ( $1548.2$ ,  $1550.8\text{\AA}$ ), and (c) Si IV ( $1393.8$ ,  $1402.8\text{\AA}$ ). Abscissae, wavelengths in Angstrom units. Ordinates, flux in relative units. Vertical lines labeled with numbers indicate the position of the possibly identified lines listed in the box.



WAVELENGTH (Å)

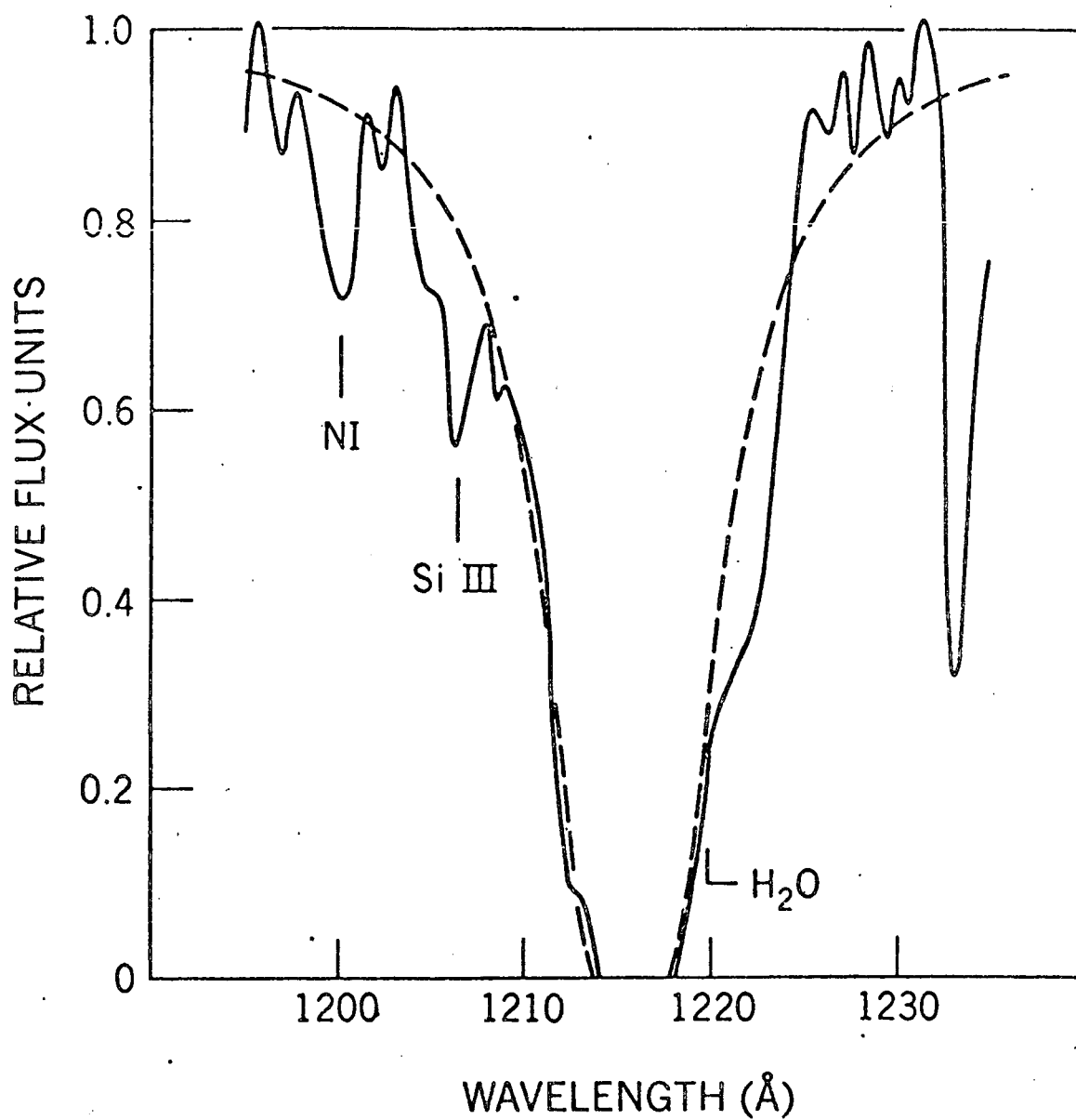


FIG. 2.

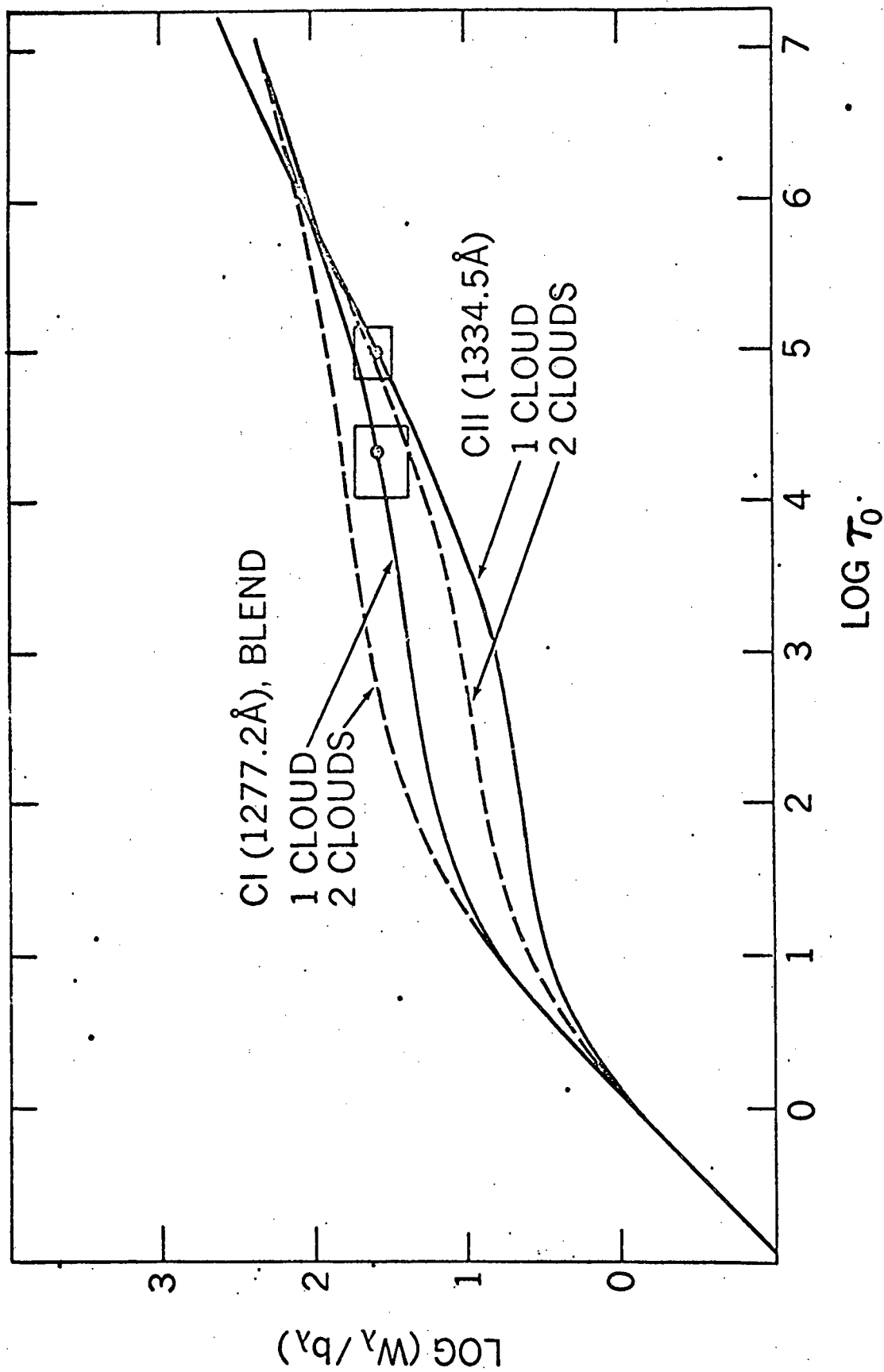


FIG. 3

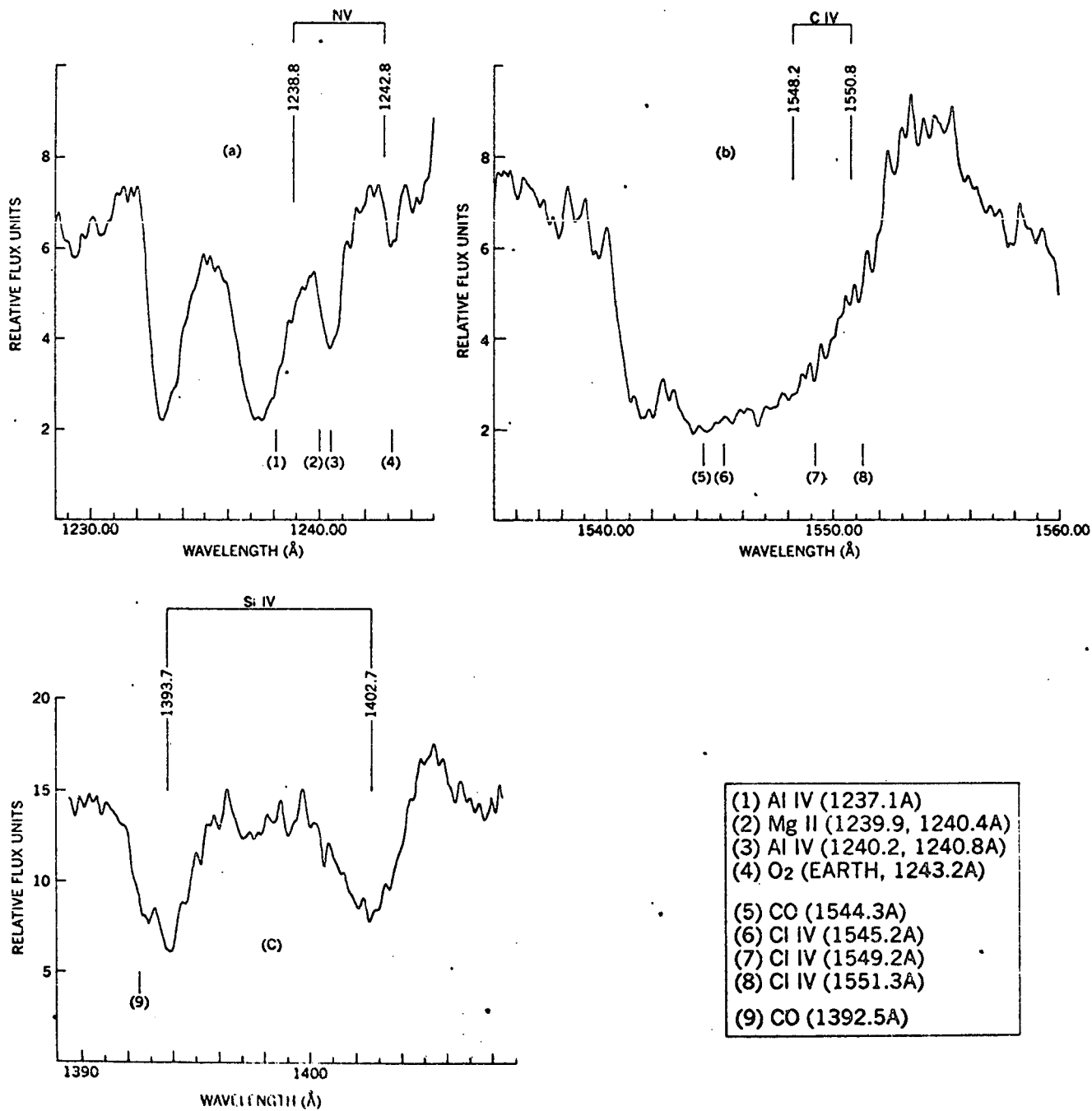


FIG. 4